Fullerenic solitons

Fullerenic solitons

Yves Brihaye[1] **and Betti Hartmann**[2]

[1] Faculté des Sciences, Université de Mons-Hainaut, 7000 Mons, Belgium
[2] School of Engineering and Sciences, International University Bremen (IUB), 28725 Bremen, Germany

E-mail: Yves.Brihaye@umh.ac.be and b.hartmann@iu-bremen.de

Abstract
We study a modified nonlinear Schrödinger equation on a two-dimensional sphere with radius R with the aim of describing electron–phonon interactions on fullerenes and fullerides. These electron–phonon interactions are known to be important for the explanation of the high transition temperature of superconducting fullerides. As in the $R \rightarrow \infty$ limit, we are able to construct non-spinning as well as spinning solutions which are characterized by the number of nodes of the wavefunction. These solutions are closely related to the spherical harmonic functions. For small R, we discover specific branches of the solutions. Some of the branches survive in the $R \rightarrow \infty$ limit and the solutions obtained on the plane ($R = \infty$) are recovered.

PACS numbers: 73.61.Wp, 11.27.+d

1. Introduction

Carbon exists in several forms in nature. One is the so-called fullerene which was discovered for the first time in 1985 [1]. Fullerenes are carbon-cage molecules in which a large number n of carbon (C) atoms are bonded in a nearly spherically symmetric configuration. These C_n configurations typically have diameters of $d \approx 7$–15 Å and consist of 12 pentagons and $\left(\frac{n}{2} - 10\right)$ hexagons, where $n \geqslant 24$ has to be even. The most prominent example is the C_{60} fullerene which is also called a 'buckminster' fullerene. It consists of 20 hexagons and 12 pentagons and has a diameter of $d_{60} \approx 7$ Å. In these fullerenes, three valence electrons of the C-atom are used to form bonds with the neighbouring C-atoms, while the remaining 'free' valence electron can 'hop' along the n positions in the fullerene.

Due to unoccupied electron orbitals, it is easy to reduce fullerenes, i.e. put extra electrons in them. It was found that if alkali metal atoms—which donate one electron each—such as rubidium (Rb), potassium (K), caesium (Cs) or sodium (Na) are put onto a C_{60} fullerene, this leads to metallic or even superconducting behaviour [2]. The transition temperature T_c of

these alkali-doped fullerenes, also called *fullerides*, is rather high for superconductors, e.g. $T_c = 33$ K for $RbCs_2C_{60}$ [3]. The superconductivity can be explained by phonon–electron interactions in the fullerides [4]. In [5] it was found that if a C_{60} or a C_{70} molecule is doped with one or two excess electrons, the additional charges accumulate nearly along an equatorial line of the molecule. The distortion in the lattice and the electron distribution was found to be polaron-like.

Recently, a modified nonlinear Schrödinger equation has been studied in the context of fullerene-related structures, the so-called nanotubes [6, 7]. These objects are graphite-like sheets rolled to form a cylinder. The carbon atoms are bonded in a hexagonal lattice on this sheet. The existence of solitons, which are created through the interaction of the 'excitation' described by a complex scalar field ψ and the lattice vibrations, was discussed. The creation of these type of solitons was introduced by Davydov in the 1970s [8] to explain the dispersion free energy transport in biopolymers. ψ is then an amide I-vibration. Here, however, we think of ψ as the wavefunction of an 'excess' electron interacting with the lattice via electron–phonon interactions. The electron could, e.g., be thought of as the valence electron of an alkali metal atom with which the fullerene is doped. The full discrete system of equations (which results from a Fröhlich-type Hamiltonian) can be approximated by the above-mentioned modified nonlinear Schrödinger equation on the two-dimensional plane.

In this paper, we study the modified nonlinear Schrödinger equation for the hexagonal lattice on a two-dimensional sphere, thus aiming at describing the electron–phonon interactions in fullerenes and fullerides. These interactions are, as mentioned previously, of particular interest for the superconductivity of the fullerides. Our model is, of course, an approximation since fullerenes consist of hexagons and pentagons. However, since (a) there are more hexagons in the C_{60} and (b) the coefficients appearing in the nonlinear Schrödinger equation do not depend strongly on the actual form of the lattice, we believe that this is a good approximation.

Finally, let us mention that studying solitons on a sphere can appear to be useful also from a mathematical point of view, as was stressed, e.g., in [9]. In the present case this appears to be true as well. In particular, we note a strong relationship between most of the various branches of solutions and the spherical harmonics.

Our paper is organized as follows: in section 2, we present the modified nonlinear Schrödinger equation on the sphere, in section 3, we discuss non-spinning solutions and in section 4 spinning generalizations. We give our conclusions in section 5.

2. Modified nonlinear Schrödinger equation on the sphere

We consider the following modified nonlinear Schrödinger equation in two dimensions [6, 10], which in dimensionless variables reads:

$$i\frac{\partial \psi}{\partial t} + \Delta \psi + ag\psi(|\psi|^2 + b\Delta|\psi|^2) = 0 \tag{1}$$

where a, b are constants with $a = 2$, $b = \frac{1}{12}$ for the square lattice studied in [10] and $a = 4$, $b = \frac{1}{8}$ for the hexagonal lattice studied in [6]. The additional term proportional to b results from both the discreteness of the lattice and the interaction between the lattice and the complex scalar field ψ ('phonon–electron' interaction). g is the ('phonon–electron') coupling constant of the system and determines the 'strength' of the nonlinear character of the equation. In particular, as can be seen from the derivation of the modified nonlinear Schrödinger equation from the discrete equations [6], the mass of the carbon atom is encoded into g.

As stated in the introduction, we will study the above equation on a two-dimensional sphere with radius R. The Laplacian operator then reads:

$$\Delta = \frac{1}{R^2}\left(\frac{\partial^2}{\partial\theta^2} + \cot\theta\frac{\partial}{\partial\theta} + \frac{1}{\sin^2\theta}\frac{\partial^2}{\partial\varphi^2}\right). \tag{2}$$

As usual, the angles are such that $\theta \in [0 : \pi]$ and $\varphi \in [0 : 2\pi]$ and $\psi = \psi(t, \theta, \varphi)$ is a complex-valued scalar field. Since we are mainly concerned with fullerenes here which consist (next to pentagons) of hexagons, we use in analogy with [6] $a = 4$ and $b = \frac{1}{8}$. The solutions of (1) can be characterized by their norm η:

$$\eta^2 = R^2 \int |\psi|^2 \sin\theta \, d\theta \, d\varphi \tag{3}$$

as well as by their energy:

$$E = R^2 \int \left(|\vec{\nabla}\psi|^2 - \frac{a}{2}g|\psi|^4 + 2bg(\vec{\nabla}|\psi|^2)^2\right)\sin\theta \, d\theta \, d\varphi. \tag{4}$$

The coupling constant g can be absorbed into the scalar field ψ by rescaling it as follows: $\psi \to \psi/\sqrt{g}$. In our numerical simulations, we will set $g = 1$. This in turn means that we drop the normalization constraint ($\eta = 1$) for the wavefunction ψ. However, since we present explicitly the norm of our numerical solutions, the normalized wavefunction and the corresponding value of g can be easily computed. In particular, if a solution ceases to exist for a specific value of the norm, this means that the soliton solution exists only above a high enough value of the phonon–electron coupling.

3. Non-spinning solutions

To construct explicit solutions, we use the following axially symmetric ansatz [11–13]:

$$\psi = e^{i\omega t}\Phi(\theta). \tag{5}$$

Inserting the ansatz into equation (1), we find

$$\Phi'' + \cot\theta\,\Phi' + \Phi'^2\frac{g\Phi}{1 + g\Phi^2} + \frac{4g\Phi^3 - \omega\Phi}{1 + g\Phi^2}R^2 = 0 \tag{6}$$

where the prime denotes the derivative with respect to θ. Note that we are fixing the length scale λ of the space variable by $R_{phy} = \lambda R$, where R_{phy} is the physical radius of the fullerene and λ is of the order of Å. We will vary R here in order to take the $R \to \infty$ limit and thus compare our results with those of [6, 7]. The other dimensionful physical quantities can be recovered by reinserting the physical constants of the model appropriately (see, e.g., equations (6), (7) of [6]). As far as the frequency ω_{phy} is concerned, we have

$$\omega_{phy} = \frac{\hbar}{2m}\frac{1}{R_{phy}^2}\omega \tag{7}$$

where m is the mass of the 'electron'. Thus, since ω is dimensionless, ω_{phy} has the dimension of an inverse time: $[\omega_{phy}] = \text{s}^{-1}$.

The regularity of the solutions at $\theta = 0, \pi$ requires the following boundary conditions:

$$\Phi'|_{\theta=0} = \Phi'|_{\theta=\pi} = 0. \tag{8}$$

For later convenience, we denote by $\mathcal{M}$ the reflection operator with respect to the equatorial ($\theta = \pi/2$) plane : $\mathcal{M}\Phi(\theta, \varphi) = \Phi(\pi - \theta, \varphi)$. We will call solutions for which $\mathcal{M}\Phi = \Phi$ symmetric, those with $\mathcal{M}\Phi = -\Phi$ antisymmetric and finally solutions for which $\mathcal{M}\Phi \neq \pm\Phi$ will be called asymmetric in the following.

It appears impossible to construct explicit solutions of (6), (8). This is why numerical techniques have to be adopted. However, in our numerical study, it became obvious that the pattern of solutions occurring for different values of ω is quite complicated. In an attempt to understand this pattern, we have analysed the linearized equation first. This analysis will be discussed prior to presenting the numerical results.

3.1. Linearized equation

First, we remark that (6) has three fixed points, repectively $\Phi_c = 0$ and $\Phi_c = \pm\sqrt{\frac{\omega}{4}}$. Perturbing around one of these fixed points according to

$$\Phi(\theta) = \Phi_c + \epsilon f(\theta) + O(\epsilon^2) \tag{9}$$

and linearizing the equation in ϵ leads to

$$f'' + \cot\theta f' - \omega R^2 f = 0 \qquad \text{if} \quad \Phi_c = 0 \tag{10}$$

and

$$f'' + \cot\theta f' + \frac{2R^2\omega}{1 + \omega/4} f = 0 \qquad \text{if} \quad \Phi_c = \pm\sqrt{\frac{\omega}{4}}. \tag{11}$$

In both cases, we recognize the equation of Legendre polynomials P_n : $P_n'' + \cot\theta P_n' + n(n+1)P_n = 0$. If we take into account the boundary conditions given by (8), the relevant solutions of the linearized equation are given in terms of these polynomials and fix a relation between R, ω and the integer n:

$$f(\theta) = P_n(\theta) \qquad \text{with} \qquad \omega R^2 = -n(n+1) \qquad \text{if} \quad \Phi_c = 0 \tag{12}$$

and

$$\tilde{f}(\theta) = P_n(\theta) \qquad \text{with} \qquad \frac{2\omega R^2}{1 + \omega/4} = n(n+1) \qquad \text{if} \quad \Phi_c = \pm\sqrt{\frac{\omega}{4}}. \tag{13}$$

In particular, the above relations define two sets of critical values of the spectral parameter ω as a function of R which are indexed by n. For (12) and (13) we find, respectively

$$\omega_{cr,n} \equiv -\frac{n(n+1)}{R^2} \tag{14}$$

$$\tilde{\omega}_{cr,n} \equiv \frac{4n(n+1)}{8R^2 - n(n+1)}. \tag{15}$$

From the above analysis, setting $n = 1$ such that $P_1 \propto \cos\theta$, we conclude that the perturbed solution about $\Phi_c = \sqrt{\omega/4}$ is positive (e.g. especially it has no nodes, at least for values of ω close to the critical values) and has a maximum above the north pole ($\theta = 0$), a minimum above the south pole ($\theta = \pi$).

The perturbed solution about $\Phi_c = 0$ leads to a solution which is antisymmetric under the reflection $\mathcal{M}$. It vanishes at the equator (i.e. has a node at $\theta = \pi/2$) and possesses a maximum above the north pole, a minimum above the south pole.

Of course, the functions presented here constitute only approximations (even up to an unfixed multiplicative constant) to the solutions of the full equation (6). The closer we are to the critical points (14) and (15), the more accurate these approximations are. Nevertheless, by performing this analyis we gain extremely useful information about the solutions of the full equations, namely about (i) their symmetries and (ii) the critical values of ω where the various branches start or finish. In the following section, we discuss the numerical results.
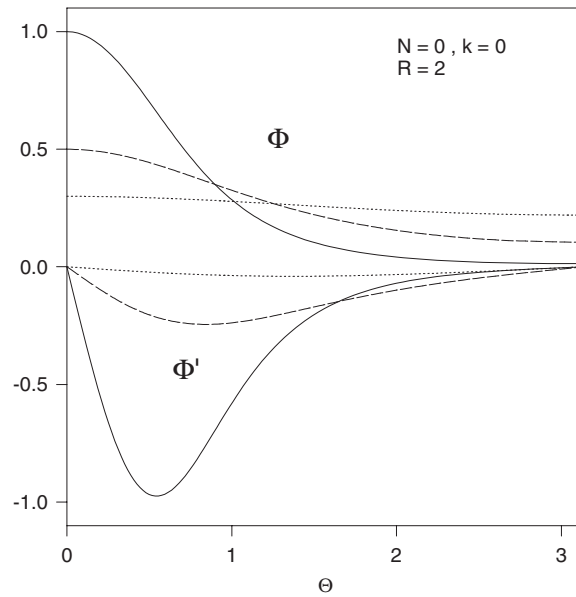
Figure 1. The profile of the non-spinning, nodeless ($N = 0, k = 0$) solution and its derivative is presented for $R = 2$ and three values of $\Phi(0)$, namely $\Phi(0) = 1.0, 0.5$ and 0.3.

3.2. Numerical results

We constructed solutions numerically for generic values of R and of ω. In our numerical routine, $\Phi(0)$ is used as a shooting parameter and the regular solution as well as the corresponding value of ω is determined numerically. We first constructed a 'fundamental' solution which has no node ($k = 0$). For generic values of the parameters, this solution corresponds to the above-mentioned deformation of the Legendre polynomial P_1 and is thus positive, has a maximum for $\theta = 0$ and a minimum at $\theta = \pi$. This is illustrated in figure 1 for $\Phi(0) = 1.0, 0.5$ and 0.3. Keeping R fixed and varying $\Phi(0)$ we obtain a branch of asymmetric solutions labelled by ω. Our numerical analysis strongly suggests that these regular solutions exist for $\tilde{\omega}_{cr,1} \leqslant \omega < \infty$ with

$$\tilde{\omega}_{cr,1} \equiv \frac{1}{R^2 - 1/4}. \tag{16}$$

In the limit $\omega \to \tilde{\omega}_{cr,1}$ the solution tends to the constant solution $\Phi = \sqrt{\tilde{\omega}_{cr,1}/4}$, which for $R = 2$ is equal to 0.2582. As can be seen in figure 1, the solution for $\Phi(0) = 0.3$ is already nearly constant and thus close to this critical solution.

In correspondence with these solutions, the mirror symmetric ones also exist and constitute another branch with the same values of ω.

Next, we constructed a family of solutions having one node for $\theta \in]0, \pi[$. The node occurs at $\theta = \pi/2$ and the solutions of this branch are antisymmetric under the reflection $\mathcal{M}$, as illustrated in figure 2. These solutions exist only for $\omega \geqslant \omega_{cr,1} \equiv -2/R^2$ and for arbitrary large values of ω. In the limit $\omega \to \omega_{cr,1}$, the solutions are of the form (9) with $\Phi_c = 0$ and $f(\theta) = \cos\theta$. This is shown in figure 2, where the solution with $\Phi(0) = 0.25$ is proportional to the trigonometric function $\cos\theta$. When ω is increased the effects of the nonlinear term become stronger and the solution's profile deviates considerably from an elementary trigonometric function.
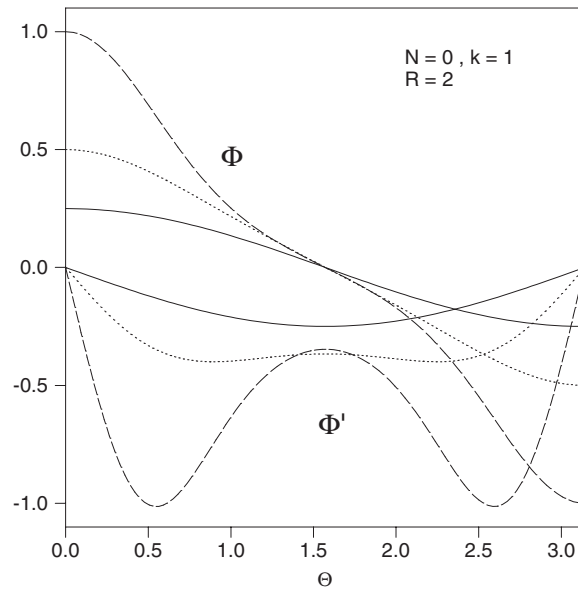
Figure 2. The profile of the non-spinning, one-node ($N = 0$, $k = 1$) solution and its derivative is presented for $R = 2$ and three values of $\Phi(0)$, namely $\Phi(0) = 1.0$, 0.5 and 0.25.

When investigating this branch of solutions for larger values of $\Phi(0)$ (or equivalently of ω) we observed that the one-node solution develops a plateau (surrounding the region $\theta = \pi/2$) on which the function Φ is very close to zero. Away from this plateau the solution resembles two disconnected solitons located at the two poles of the sphere. This is illustrated in figure 3 (solid line) for $\Phi(0) = 3.7$ and the corresponding value of ω is 15.95. However, for large enough values of $\Phi(0)$, i.e. of ω, our numerical analysis strongly indicates that *asymmetric* solutions exist next to the antisymmetric ones described above. In figure 3 such an asymmetric solution corresponding to $\omega = 14.85$ together with a comparable antisymmetric solution is presented. The asymmetric solution in figure 3 (dotted line) has an energy of order -900 (in our dimensionless variables). This has to be contrasted with the energy of the antisymmetric solution (solid line) which is of order -300. This result is interesting in view of [5]. There, it was found that the excess electron density in the C_{60} fullerene is located along an equatorial line of the C_{60}. The excess electron density here can be represented by $\Phi^2(\theta)$. We find here, that the solution with the electron density located at the equator (asymmetric solution) is energetically more favourable than the one which has the electron density located in one of the hemispheres. It is remarkable that the two solutions show a very similar behaviour around $\theta = 0$ and start to deviate from each other at roughly $\theta > 0.8$. Unfortunately, this similarity of the solutions in the region around the north pole renders the numerical construction of the solutions extremely difficult. This is why we did not succeed in constructing the full asymmetric branch. However, let us mention that a similar feature occurs as well in the spinning case $N = 1$. In this case, the numerical analysis was much easier and we will thus discuss this point again in the section about spinning solutions.

The values of the norm η, the energy E and the value $\Phi(0)$, which corresponds to the maximal value of the solution, are shown in figure 4 as functions of ω for both the fundamental ($k = 0$) and the one-node ($k = 1$) solution with $R = 2$ (the graph is limited to $\omega \leqslant 1.5$).
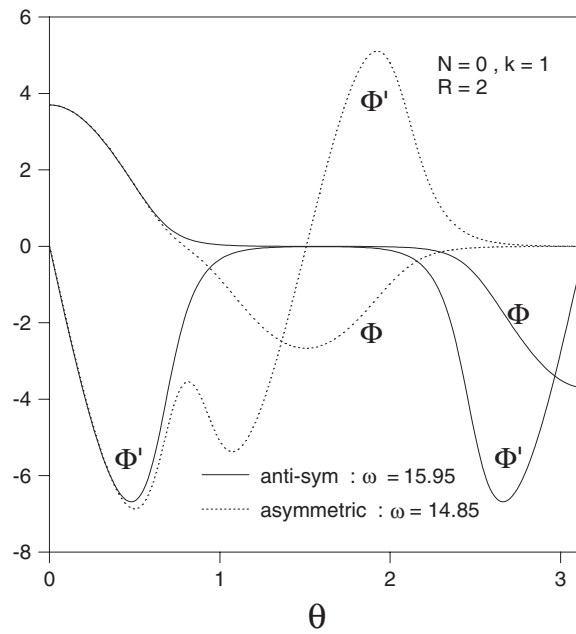
Figure 3. The profile of one solution on the antisymmetric branch (corresponding to $\omega = 15.95$) as well as one solution on the asymmetric branch (corresponding to $\omega = 14.85$) is shown for $N = 0, k = 1$ and $R = 2$. The corresponding derivatives of the solutions are also shown.
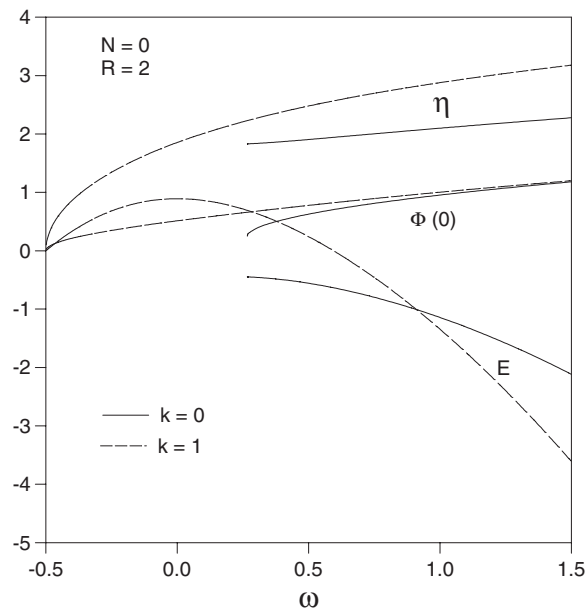

Figure 4. The values of the energy E, the norm η and of $\Phi(0)$ are shown as functions of ω for the fundamental ($k = 0$) and one-node ($k = 1$) solutions with $N = 0$ (non-spinning) and $R = 2$.

Solutions having more nodes of the function $\Phi(\theta)$ can be constructed in correspondence with the higher order Legendre polynomials. However, the systematic study of these solutions is not the aim of this paper.

Finally, we remark that

$$\lim_{R\to\infty} \omega_{cr,1} = \lim_{R\to\infty} \tilde{\omega}_{cr,1} = 0. \tag{17}$$

This is in agreement with [7], and confirms that in the plane both fundamental and one-node solutions can be constructed for $\omega \geqslant 0$.

4. Spinning solutions

In order to construct spinning solitons, we use the ansatz [12, 13]:

$$\psi = e^{i\omega t + iN\varphi} \Phi(\theta) \tag{18}$$

which, after inserting into (1), leads to the equation

$$\Phi'' + \cot\theta\, \Phi' + \Phi'^2 \frac{g\Phi}{1+g\Phi^2} + \frac{4g\Phi^3 - \omega\Phi}{1+g\Phi^2} R^2 - \frac{N^2}{1+g\Phi^2} \frac{1}{\sin^2\theta} \Phi = 0. \tag{19}$$

Regularity of the solutions at $\theta = 0, \pi$ requires

$$\Phi(0) = \Phi(\pi) = 0. \tag{20}$$

In this case, $\Phi_c = 0$ is the only fixed point of the equation and the corresponding linearized equation is solved by the associated Legendre functions P_n^N, $-n \leqslant N \leqslant n$, provided that relation (14) holds. In what follows, n will be related to the number k of nodes of the solution by $k = n - N$.

We would like to mention that we were able to construct an exact solution of the above equation for $N = 1$ and $R^2 = 3/4$. It is of the form

$$\Phi = \alpha \sin\theta \qquad \text{with} \quad \omega = \frac{8(\alpha^2 - 1)}{3} \tag{21}$$

where α is a real constant. Obviously, this solution is symmetric.

4.1. Numerical results for $N = 1$

In this case, the numerical solutions can be constructed by using the value $\Phi'(0)$ as a shooting parameter. We studied numerically the solutions corresponding to the deformation of the associated Legendre function $P_1^1 \propto \sin\theta$ (for no-node solutions) and of $P_2^1 \propto \sin\theta \cos\theta$ (for one-node solutions) and found that in accordance with (14), there exist no solutions for respectively

$$\omega \leqslant -\frac{2}{R^2} \equiv \omega_{cr,1} \qquad \omega \leqslant -\frac{6}{R^2} \equiv \omega_{cr,2}. \tag{22}$$

As for the case of non-spinning solution, the norm η, the energy E and the parameter $\Phi'(0)$ are presented in figure 5.

As can be seen from this figure, a new phenomenon occurs in the case of spinning solutions without nodes. Namely, the main branch corresponding to the deformation of P_1^1 stops at some critical value of ω, say $\omega_{\max}$ with $\omega_{\max} > \omega_{cr,1}$ (for $R = 2$, we find $\omega_{\max} \approx 0.3$). However, the inspection of figure 5 by no means reveals that some critical phenomenon occurs in this limit. When plotting the quantities E, ω and the norm η as functions of the shooting parameter $\Phi'(0)$ (see figure 6), though, it is clearly indicated that some critical phenomenon appears. Indeed as our numerical results indicate, the slope of the curves becomes infinite when the shooting
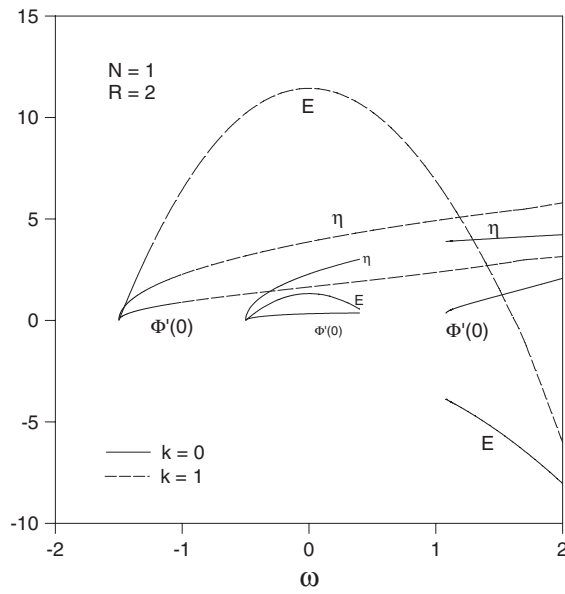
Figure 5. The values of the energy E, the norm η and of $\Phi'(0)$ are shown as functions of ω for the fundamental ($k = 0$) and one-node ($k = 1$) solutions with $N = 1$ (spinning) and $R = 2$.
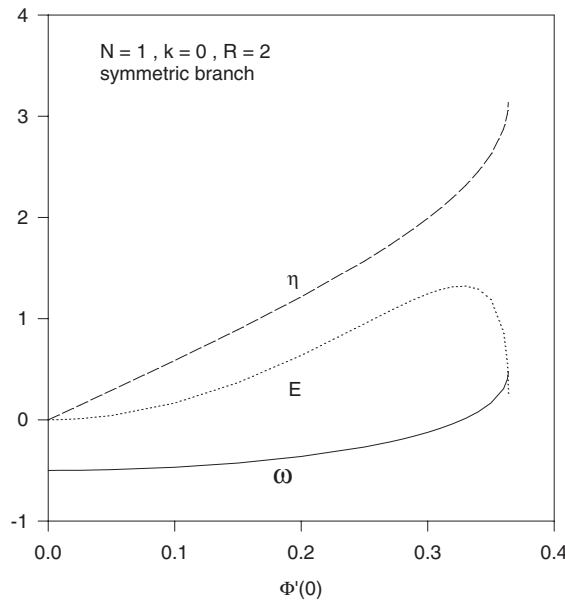

Figure 6. The values of the energy E, the norm η and of ω are shown as a function of $\Phi'(0)$ for the spinning, nodeless ($N = 1, k = 0$) solutions with $R = 2$.

parameter reaches the critical point. The solutions on this branch are symmetric under the operator $\mathcal{M}$. The profile of the symmetric solution corresponding to $\Phi'(0) = 0.25$ is shown in figure 7.
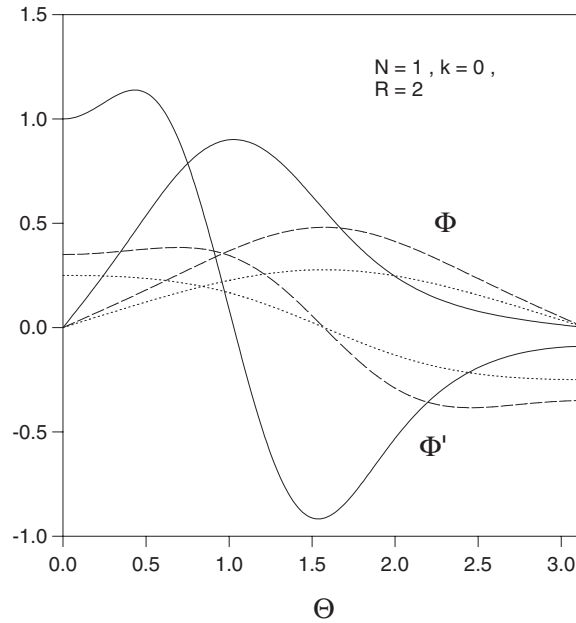
Figure 7. The profile of the spinning, nodeless ($N = 1$, $k = 0$) solution and its derivative is shown for $R = 2$ and three values of $\Phi'(0)$, namely $\Phi'(0) = 1.0$, 0.36 and 0.25.

Table 1. Critical values of ω for different R.

R	$\omega_{cr,1}$	ω_{max}	$\bar{\omega}$
∞	0	0	0
5	$-2/25$	0.03	0.15
2	$-1/2$	0.3	1.0
1.5	$-2/(1.5)^2$	1.3	2.15
$\sqrt{3/4}$	$-3/8$	∞	∞

For sufficiently large values of ω, say $\omega > \bar{\omega}$ ($\bar{\omega} \approx 1.0$ for $R = 2$), a new branch of nodeless solutions appears which seems to exist for arbitrary large values of ω, while for $\bar{\omega} > \omega > \omega_{max}$ no solutions seem to exist at all.

The solutions for $\omega > \bar{\omega}$ are asymmetric under the reflection $\mathcal{M}$. Only the limiting solution at $\omega = \bar{\omega}$ is symmetric under $\mathcal{M}$. An asymmetric solution corresponding to $\Phi'(0) = 1.0$ as well as the limiting, symmetric solution for $\Phi'(0) = 0.36$ is shown in figure 7. Clearly the asymmetry increases with increasing $\Phi'(0)$. In other words, when $\omega > \bar{\omega}$ increases, the wavefunction of spinning, nodeless solitons is more and more concentrated in one of the hemispheres.

All the above results were obtained for $R = 2$. However, we also studied the dependence of the critical values of ω on the radius R of the sphere. The results are given in table 1.

For a generic value of R such that $\sqrt{3/4} < R < \infty$ two branches of solutions exist, namely a branch of symmetric solutions for $\omega \in [\omega_{cr,1} : \omega_{max}]$ and a branch of asymmetric solutions for $\omega \in [\bar{\omega} : \infty]$. In the limit $R \to \infty$, the symmetric branch disappears and only the asymmetric one survives. In the limit $R \to \sqrt{3/4}$ only symmetric solutions seem to exist since $\bar{\omega} \to \infty$. In this respect, the explicit solution (21) plays a major role.
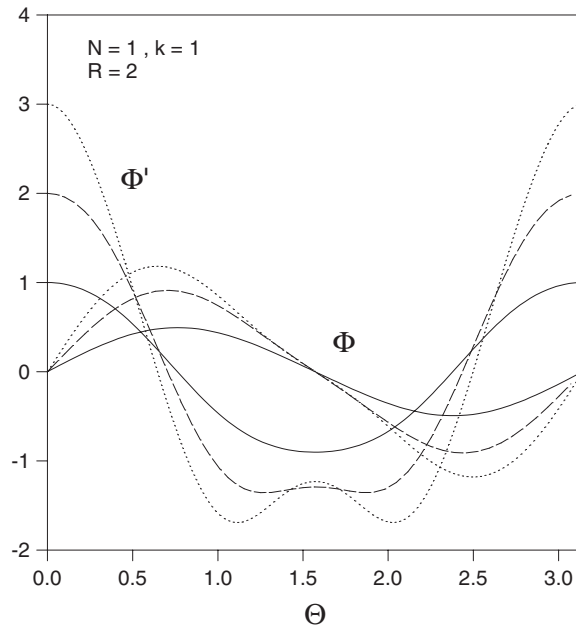
Figure 8. The profile of the spinning, one-node ($N = 1, k = 1$) solution and its derivative is shown for $R = 2$ and three values of $\Phi'(0)$, namely $\Phi'(0) = 3.0, 2.0$ and 1.0.

Finally, we constructed one branch of spinning, one-node solutions. They exist for $\omega \geqslant -6/R^2 \equiv \omega_{cr,2}$ and are symmetric under the operator $\mathcal{M}$. They vanish when ω approaches the lower critical limit $\omega_{cr,2}$ and seem to exist for arbitrary large values of ω. Spinning, one-node solutions corresponding to $\Phi'(0) = 1.0, 2.0$ and 3.0 are shown in figure 8.

4.2. Numerical results for $N = 2$

We have also constructed spinning solutions corresponding to $N = 2$. The solutions are deformations of the associated Legendre functions $P_2^2 \propto 1 - \cos(2\theta)$ (for no-node solutions) and $P_3^2 \propto \cos\theta - \cos(3\theta)$ (for one-node solutions). In agreement with the analysis of the linearized equation, no solutions exist respectively for

$$\omega \leqslant -\frac{6}{R^2} \equiv \omega_{cr,2} \qquad \omega \leqslant -\frac{12}{R^2} \equiv \omega_{cr,3}. \tag{23}$$

Furthermore, the no-node solutions are symmetric under $\mathcal{M}$, while the one-node solutions are antisymmetric under $\mathcal{M}$. No branch of asymmetric solutions seems to exist in this case. Thus, as far as our numerical analysis indicates, in contrast to the $N = 1$ case, these are the only $N = 2$ solutions for $n \leqslant 3$.

5. Conclusion

The study of the modified nonlinear Schrödinger equation of [6, 7, 10] on the sphere reveals a very rich set of stationary solutions. They can be characterized by their behaviour under the reflection operator $\mathcal{M}$ with respect to the equator ($\theta = \pi/2$) plane. We constructed branches of solutions which are either (i) symmetric under $\mathcal{M}$, (ii) antisymmetric under $\mathcal{M}$ or (iii)

asymmetric under $\mathcal{M}$. The solutions are further characterized by their spinning number N and the number of nodes k of the wavefunction which we find—as expected—to be closely related to the quantum numbers of the spherical harmonics. Linearizing the modified nonlinear Schrödinger equation, we find that the lower value of ω, above which solutions exist, is determined by the spectral parameters obtained from the linearized equation.

An unexpected phenomenon occurs in the cases $N = 0, k = 1$ and $N = 1, k = 0$. For $N = 0, k = 1$, we find that for comparable values of ω two branches of solutions exist: one of which is antisymmetric and one which is asymmetric. For $N = 1, k = 0$, we observe that for finite $R > \sqrt{3/4}$ the symmetric solutions only exist on a finite interval of the parameter ω. Since ω is related to the kinetic energy of the solution [7], this means in other words that only for solutions with sufficiently low kinetic energy is the probability density of the 'electron' the same in both hemispheres. If the kinetic energy becomes large enough, the electron density is essentially concentrated in one of the hemispheres. In [5], it was found that the excess electron density in fullerides is located around the equator. Here, we find $\Phi^2(\theta)$ to be concentrated around the equator in two cases: (a) for the $N = 0, k = 1$ case if ω is large enough, (b) for $N = 1, k = 0$ if $\omega \in [\omega_{cr,1}(R) : \omega_{\max}(R)]$.

We have not studied $N > 2$ and/or $k > 1$ in this paper. We believe that the above-mentioned properties also hold true for these type of solutions and that, in particular, the solution with N, k is related to the associated Legendre function P_{k+N}^N.

Acknowledgments

References

[1] Kroto H W, Heath J R, O'Brien S C, Curl R F and Smalley R E 1985 *Nature* **318** 162
[2] Haddon R C *et al* 1991 *Nature* **350** 320
    For a review, see Gunnarsson O 1997 *Rev. Mod. Phys.* **69** 575
[3] Tanigaki K, Ebbesen T W, Saito S, Mizuki J, Tsai J S, Kubo Y and Kuroshima S 1991 *Nature* **352** 222
[4] Varma C M, Zaanen J and Raghavaclari K 1991 *Science* **254** 989
    Schluter M A, Lannoo M, Needles M, Baraff G A and Tomanek D 1992 *Phys. Rev. Lett.* **68** 526
    Schluter M A, Lannoo M, Needles M, Baraff G A and Tomanek D 1992 *J. Phys. Chem. Solids* **53** 1473
    Mazin I I, Rashkeev S N, Antropov V P, Jepsen O, Lichtenstein A I and Andersen O K 1992 *Phys. Rev.* B **45** 5114
[5] Harigaya K 1992 *Phys. Rev.* B **45** 13676
[6] Hartmann B and Zakrzewski W J 2003 *Phys. Rev.* B **68** 184302 (*Preprint* cond-mat/0304181)
[7] Brihaye Y, Hartmann B and Zakrzewski W J 2003 Spinning solitons of a modified nonlinear Schrödinger equation *Preprint* hep-th/0308155
[8] Davydov A S 1985 *Solitons in Molecular Systems* (Dordrecht: Reidel)
    Scott A 1992 *Phys. Rep.* **217** 1
    Scott A 1996 *Nonlinear Excitations in Biomolecules* ed M Peyrard (Berlin: Springer)
[9] de Innocentis M and Ward R S 2001 *Nonlinearity* **14** 663
[10] Brizhik L, Eremko A, Piette B and Zakrzewski W J 2003 *Nonlinearity* **16** 1481
[11] Coleman S 1985 *Nucl. Phys.* B **262** 263
[12] Schunck F E and Mielke E W 1996 *Relativity and Scientific Computing* (Berlin: Springer) p 138
[13] Volkov M and Wöhnert E 2002 *Phys. Rev.* D **66** 085003